IN THE UNITED STATES PATENT AND TRADEMARK OFFICE

APPLICANT(s):	Sonti, et al.	CONF. NO.:	3267
SERIAL NO.:	10/802,141	ART UNIT:	1742
FILING DATE:	03/17/2004	EXAMINER:	Kessler, Christopher S.
TITLE:	METHOD AND APPARATUS FOR STRENGTHENING OF POWDER METAL GEARS BY AUSFORMING		
ATTORNEY DOCKET NO.:	215P011709-US (PAR)		

Declaration Under 37 C.F.R. 1.132

I, Dr. Nagesh Sonti being as listed an inventor in the subject patent application do hereby state that:

1. I, Nagesh Sonti, have over nineteen years of experience in the design and production of gears. In addition, I have over thirty three years of experience in thermal-mechanical processing of steels, including heat treatment, joining, machining and finishing of steel components. I am presently a Research Engineer at the Applied Research Lab at Pennsylvania State University. I have a Ph.D. in Engineering Science and Mechanics from Pennsylvania State University, a Masters degree in welding engineering from Ohio State University and a Bachelors degree in mechanical engineering from the University of Madras, India.

2. Surface durability tests were conducted at the Applied Research Lab at Pennsylvania State University to compare the pitting fatigue resistance of wrought steel gears; powder metal

forged (fully densified) steel gears; and ausformed powder metal forged steel gears.

3. As a result of the tests the Ausformed powder metal forged gears showed:

about a 100% higher pitting fatigue G-50 life as compared to wrought steel gears, and

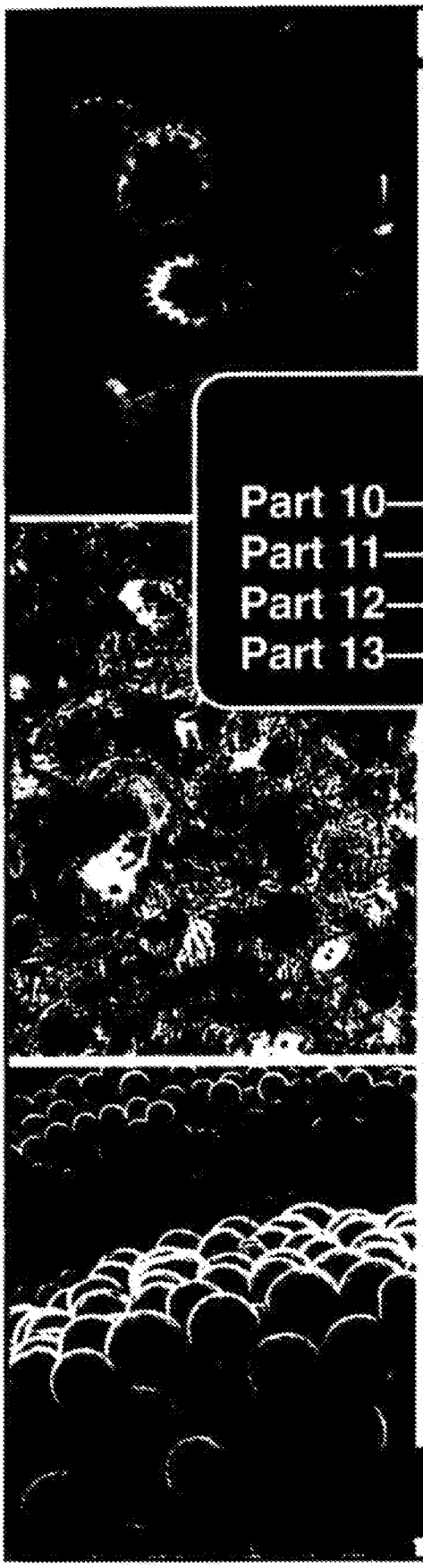
a pitting fatigue G-50 life of over ten times higher than powder metal forged steel gears that had not been ausformed.

4. The exceptionally better performance of ausformed powder metal steel gears can be attributed to the enhanced accuracy and surface finish of ausformed powder metal gears, as well as increased strength due to ausforming effects.

And, further, that all statements made herein based on our knowledge are true and that all statements made on information and belief are believed to be true, and that we are aware that willful false statements and the like are punishable by fine or imprisonment, or both (18 U.S.C. 1001), and may jeopardize the validity of this application, document, or patent issuing therefrom.

S Nagesh Dated: 12-12-2007

Dr. Nagesh Sonti



ADVANCES in Powder Metallurgy & Particulate Materials—2005

Volume III

Part 10—Material Properties
Part 11—Test & Evaluation
Part 12—Applications
Part 13—Management Issues

PM²TEC2005
JUNE 19-23 • MPIF
Montréal

Compiled by:
Candido Ruas
Ted A. Tomlin

Evaluation of the Scuffing Resistance of Powder Metal Gears in the FZG Back to Back Test Rig

Joel Mandel, Gary Draxler, and Timothy Geiman
GKN Sinter Metals, Germantown, WI

Presented at PM²TEC2005
International Conference on Powder Metallurgy & Particular Materials
June 19-23, 2005 Montreal, Quebec, Canada

ABSTRACT

The continual improvement in powder metallurgy (P/M) processes and materials have resulted in a new class of high performance, and high precision components. One product line that is generating significant interest is P/M gearing, as applied to automotive transmissions, power tools, and lawn and garden equipment. In order to expand applications further, one significant hurdle that the P/M industry must overcome is the lack of performance data for P/M materials in gear applications. Comparisons between the textbook data of traditional wrought gear materials, such as carburized 8620, and P/M have not been able to explain why P/M gears frequently outperform wrought material gears even when property data indicates otherwise.

This paper first describes the history of and current approaches to gear testing, and how the FZG back-to-back tester can be applied for the generation of P/M gear performance data. The initial results of a long-term research program that will evaluate and compare the scuffing resistance of powder metal gears made by a range of processes to the baseline performance of carburized 8620 gears will also be described. The paper will explain the test setup, procedure for testing, and test results. Analysis will include stress calculations, failure modes, and microstructural evaluation.

INTRODUCTION

Historically, the most common method for development of a gear design and the establishment of gear materials specifications is to perform the traditional gear stress calculations[1]. Inherent to these equations are many "factors" which are estimates for safety, tooth geometries, and other design considerations for gear systems. These factors can greatly affect the safety margin of the gear design in question. Depending on the equations chosen and the factors selected, these calculations can lead to gear materials' overspecification – even when only wrought materials are considered. When used conservatively, traditional gear calculations could easily double the required material properties for a given gear set. Given the current pressures to reduce component costs and at the same time to increase performance at reduced weight, an engineering

approach that typically results in overspecification requires rethinking. The limitations of the traditional gear design approach combined with the absence of meaningful data on the performance of P/M gears is at least partially responsible for the hesitance of gear designers to consider P/M materials for heavy duty applications

This paper is the first in a series that describes the application of an established gear testing method – the Forschungstelle fur Zahnrader und Getriebebau (FZG) back to back test – to powder metal gears made by the full spectrum of processes and from several alloys. In order to facilitate the comparison of the P/M results to wrought materials, the performance of carburized 8620 was utilized as a baseline.

THE HISTORY OF POWDER METAL GEAR TESTING

When a literature search is performed on powder metal gear testing, there are very few meaningful published results available on the performance of actual P/M *gears* in comparison to competing processes. It is believed that this is one major reason why confidence in P/M gears for difficult applications is not higher. Historically, testing of P/M gears has focused on simple methods intended to assess the very basic suitability of a specific gear design and material for a given application. Typical tactics involve single tooth tests to assess toughness[2], strength, or fatigue[3,4]. In most cases the samples tested were actual gears in the as-supplied condition. Figure 1 illustrates one example of a single tooth gear test fixture that can be adapted for various test purposes.

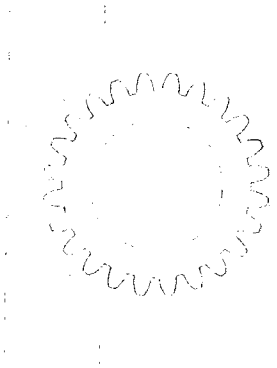


Figure 1: Typical single tooth gear testing fixture

As the core density of P/M processes increased[5,6,7], the testing focus began to change to methods intended to assess the surface durability of candidate P/M gear materials[8,9]. Rolling contact (RCF) evaluation of cylindrical P/M specimens is one common tactic to assess whether material and processing combination is potentially suitable for gear applications[10,11,12]. RCF evaluations are used to determine a material's resistance to pitting by way of an idealized test. The RCF value is used in traditional gear equations to determine the pitting resistance of gear sets. An extremely important point is the effect of the surface condition of the RCF specimen or of a P/M gear on RCF results, gear calculations, and actual P/M gear performance. Typically, RCF tests are conducted with machined specimens, which will likely have varying degrees of closed surface porosity depending on the specimen material characteristics and chosen machining method. The closed surface porosity can lead to misleading results during RCF testing. One previous study

showed the effect of porosity on RCF, and showed that the open porosity improves RCF resistance[13].

The ideal gear testing method will utilize samples with a surface condition that matches that which will be used in the intended application. For gears intended for modest duty levels, this will mean surfaces in the as-sintered or as-sized condition. For heavier duty applications, selectively densified or forged surfaces will be required. If any additional processes are needed to improve dimensional precision after heat treatment, these same processes should be applied to the test samples.

THE FZG TEST RIG

The FZG test rig is commonly used to test scuffing load capacity, pitting resistance, tooth load carrying ability, and high wear applications of gears[14]. This test can also be used to generate S-N data. Experiments are based on a standard gear set, in this case P/M and wrought gears of a predetermined geometry. Gears are tested on a machine similar to that illustrated in Figure 2.

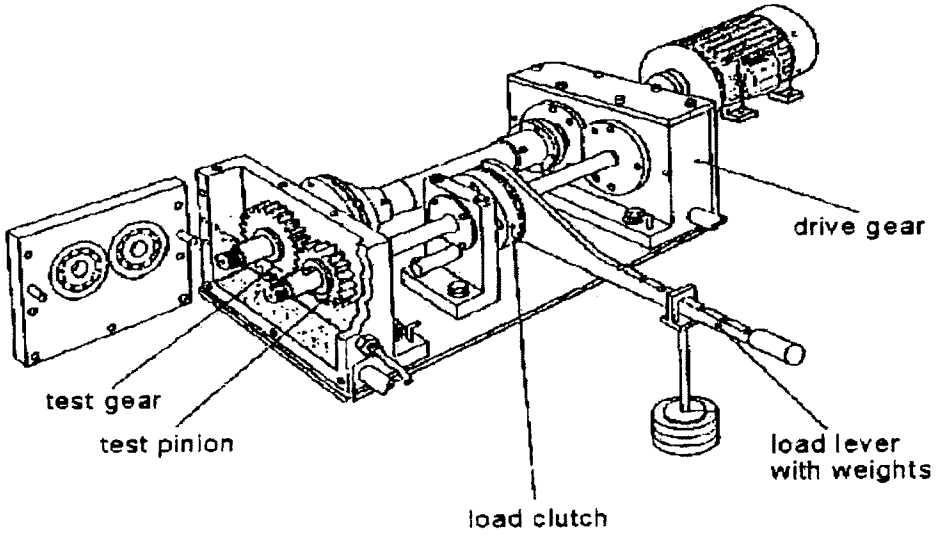


Figure 2: Schematic of the FZG Test Rig

The test rig contains a set of test gears and a set of drive gears of the same tooth geometry / tooth count. The test gears are loaded on the open end of the machine, and there is a closed loop power cycle. The two parallel shafts are connected to each other by the gears on both ends of the shaft. The torque is applied via a split shaft coupling (load clutch). The coupling allows torque to be applied to the shafts which in turn applies torque to both sets of gears. Once torque is applied, the split shaft coupling is tightened and the torque remains in the system. The motor then turns the shaft, and the gears are run at the preloaded torque. This method of testing reduces the need for a brake or other friction device to apply torque to the gears which eliminates power losses due to braking. This allows for a smaller amount of input power to compensate for losses in the system.

The torque is applied using predetermined load intervals, and the test is run for a predetermined number of cycles. These test conditions are summarized in ASTM D5182 – 92 and are summarized in Table 1.

Table 1: FZG test conditions

Load Stage	Torque on Pinion (N-m)	Tooth Normal Force (N)	Hertzian Contact Pressure (N/mm2)
1	3.3	101	124
2	13.7	421	254
3	35.3	1084	407
4	60.8	1867	535
5	94.1	2890	665
6	135.5	4161	798
7	183.4	5632	928
8 - X	239.3	7349	1061

In the case of this test, the constants of the test were the oil used, test gear geometry, speed of test, and load levels. The gears were run under identical conditions to determine the failure mode of various materials. These initial tests were used to compare materials and ranking in relative terms versus cycles to failure and failure mode.

Each load stage runs for a total of 21,700 revolutions of the pinion. After load stage 4, the gears are inspected for tooth wear, spalling, or tooth breakage. Failure is considered when the summed total of damage on all the teeth is equal to or greater than one gear tooth width. In some cases after load stage 8, the gears did not show signs of failure. The gears were then subjected to stage eight testing until failure occurred. This is then reported as the failure stage. As an example, if a gear was to run through load eight three times prior to failure, the load stage at failure would be labeled as 8-3 failure.

Test Samples for FZG Testing

The test samples used in the trial were standard test gears of the geometry shown in Table 2 Figure 3 shows the finished gears. This geometry is based on the CPMT gears which were evaluated for single tooth bending fatigue (STBF).

Table 2: Test gear data

Diametral Pitch (1 / in.)	8	
Nominal Pressure Angle (deg)	20	
Module (mm)	3.175	
Base Pitch (mm)	9.373	
Profile Contact Ratio	1.319	
	PINION	DRIVEN
Number of Teeth	20	24
Outside Diameter (mm)	71.920	84.620
Effective Outside Diameter (mm)	70.690	84.133
Reference Pitch Diameter (mm)	63.500	76.200
Normal Tooth Thickness at Ref PD (mm)	5.461	5.728
Start of Active Profile (mm)	61.109	74.199
Maximum Specific Sliding Ratio	1.793	1.338

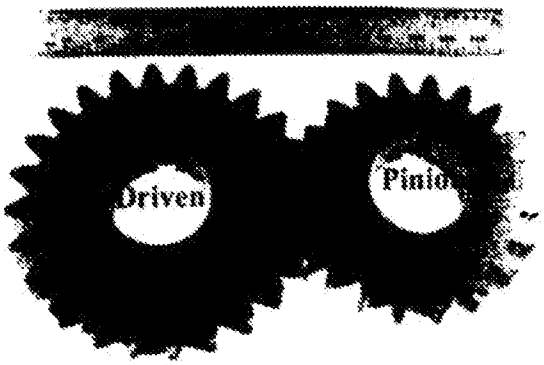


Figure 3: Test gears

FAILURE MODES OF GEARS

The two most common failures of gears are as follows[15]:

Tooth breakage due to loading of the teeth during normal operation. The tooth root is subjected to bending stress from the loading on the tooth. During normal usage and testing, this breakage can be caused from overloading or fatigue. Figure 4 shows typical tooth failure of a test gear.

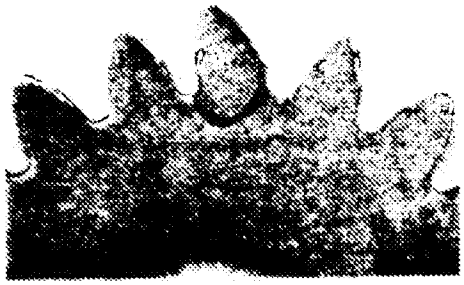


Figure 4: Tooth failure of test gear

Tooth Surface Fatigue – This is caused when the force of loading on one tooth is transferred to another tooth by intimate contact. The load area moves up and down the gear tooth profile as the gear and the pinion proceed through the mesh. Figure 5 shows typical surface fatigue failure.

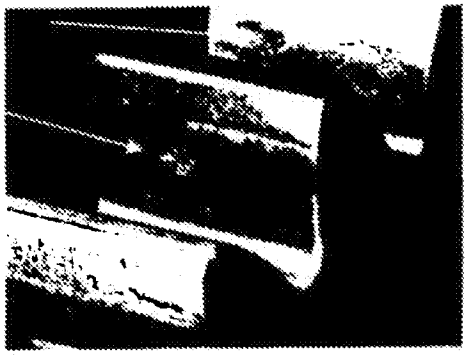


Figure 5: Tooth surface fatigue failure - pitting

Also during gear usage, the teeth may exhibit plastic flow. This is caused by the surface yielding under heavy sliding load which is indicated by rippling, ridging, rolling and peening. Although gears may exhibit this phenomena, it is not considered failure unless the flow is allowed to progress. This is common in case carburized gears, and also non heat treated or improperly heat treated gears. This can be evaluated by gear tooth measurement on a Klingelnberg (Figure 6) or similar gear measurement machine and by microstructure investigation. In the microstructure, this would be observed as surface flow or densification.

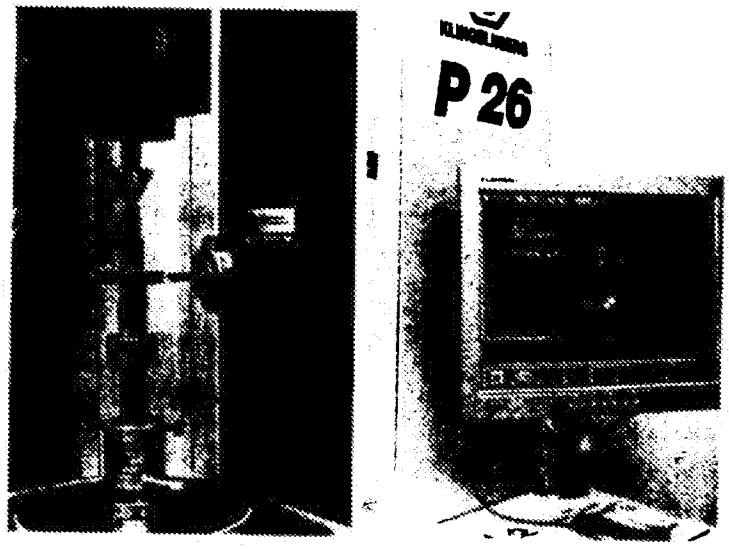


Figure 6: Gear measurement

STRESS CALULATIONS AND EVALUATION

The primary failure modes in gears are surface wear and tooth failure. Tooth failures occur primarily due to fatigue and secondly through overload. There is a fairly even distribution of surface fatigue due to pitting, spalling or a combination of the two.

AGMA has published standards for the calculation of hertzian and sliding stress for gear tooth interaction. These calculations are based on the material properties and the gear form along with numerous factors intended to encompass many variables affecting the gear performance. As stated previously, these factors can influence the gear design greatly.

To simplify the basic calculations for tooth bending stress the Lewis Formula may be used. This equation assumes the location of the maximum stress to be at a location approximately halfway up the tooth root radius. Sample calculations based on the Lewis Formula are shown in Figure 7. These sample calculations are based on a specific set of P/M material properties and the specific gear geometry used for testing. The loading is based on the load levels in the ASTM Standard D5182-97.

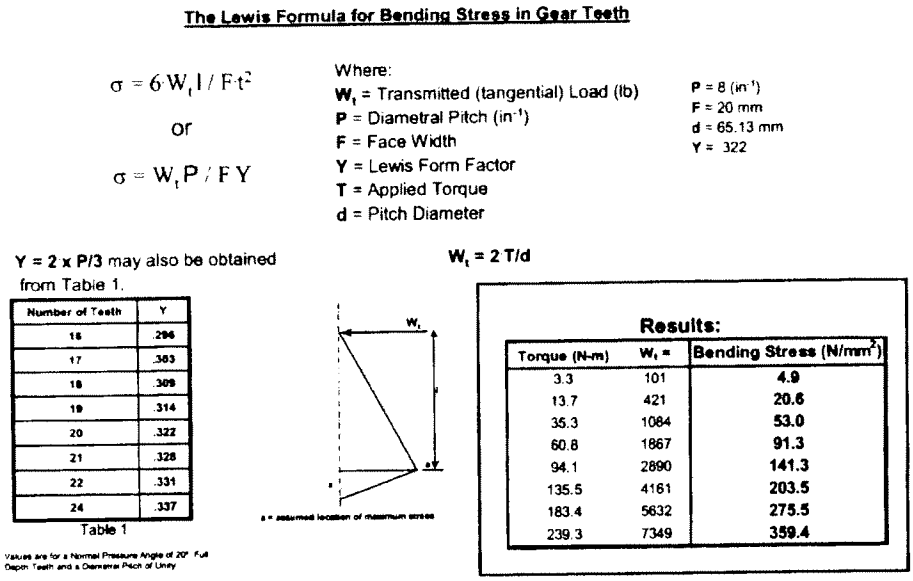


Figure 7: Sample calculation of Lewis Formula

The location of the maximum stress determined from the Lewis formula matches quite closely by an exploratory FE analysis.

Figure 8 shows the location of the maximum stress at a point approximately at the midpoint of the tooth root radius. This is where tooth breakage occurred in these tests.

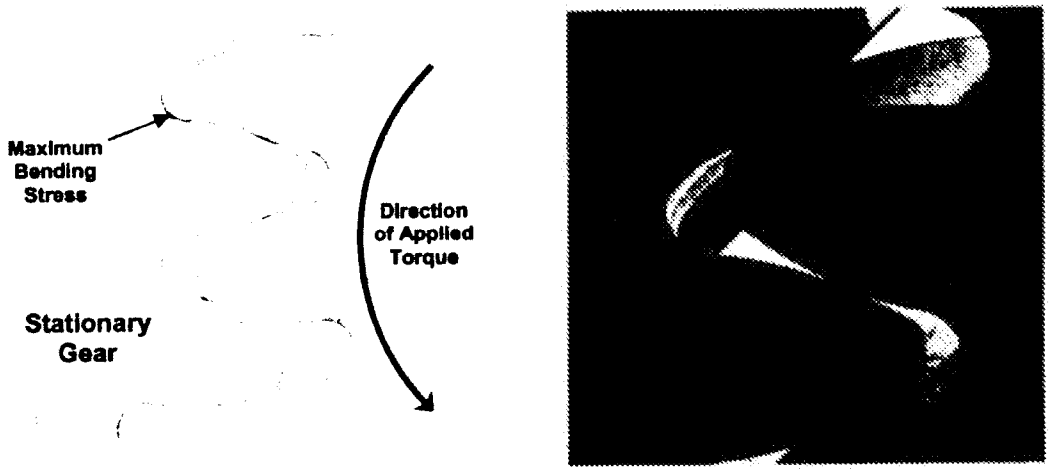


Figure 8: Bending stress at tooth root

The calculations for contact stresses may also be simplified to a static cylindrical contact situation. This assumes that no sliding is taking place, as is the case at the pitch diameters, and that the radii of curvatures of the tooth flanks can be determined at the line of contact. Examples of these calculations are shown in Figure 9. Figure 10 shows the contact pressure FEA. The spalling seen on the PM gear occurred in this area of the pitch diameter.

Maximum Contact Pressure

(Based on Cylindrical Contact Equations)

$P_{max} = 2F/\pi b l$ F = Applied Load

l = Face Width

b = ½ the width of the area in contact

$$b = \left[\frac{2F}{\pi l} \left\{ \frac{(1-\nu_1^2)}{E_1} + \frac{(1-\nu_2^2)}{E_2} \right\} \left(\frac{1}{d_1} + \frac{1}{d_2} \right)^{-1} \right]^{.5}$$

$E_1 = E_2 = 127{,}553$ MPa

$\nu_1 = \nu_2 = .28$

$r_1 = 15.55$ mm

$r_2 = 13.4$ mm

l = 20 mm

Figure 9: Contact pressure calculation

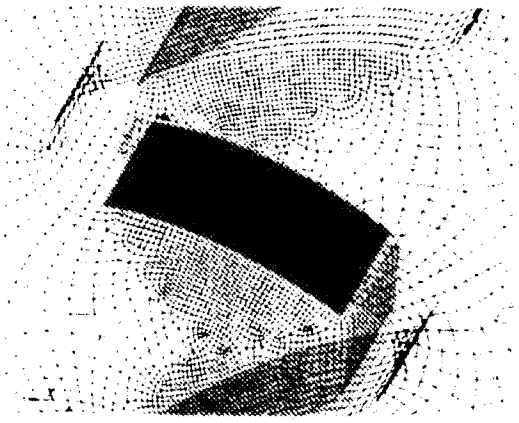


Figure 10: Typical FEA showing contact pressure location on tooth face

Materials Evaluated

One wrought material applied to heavy-duty gears is AISI 8620 steel in the carburized condition. This is the baseline material to which powder metal gears were compared. The 8620 gears were hobbed from bar stock, followed by grinding and carburizing. The powder metal parts were pressed, sintered, and then tempered per the details in Tables 3 and 4. No additional machining of the gear profile was done to the P/M gears.

Table 3: Composition of P/M Materials tested

Mix Composition				
Base Iron	**Base Iron Composition**	**Admixed Ni (wt %)**	**Admixed Cu (wt %)**	**Admixed C (wt %)**
Ancorsteel 4600V	1.75 Ni + 0.5 Mo	1	1	0.95
Ancorsteel 737SH	1.4 Ni +1.25 Mo + 0.42 Mn	0	2	0.90
Ancorloy 2	0.55 Mo	1.75*	1.5*	0.90
Ancorsteel 85HP	0.85 Mo + 0.12 Mn	0	0	0.55

*Bonded to base iron

Table 4: Processing and properties of materials tested

Material	Sintering	Heat Treat	Density (g/cc)	Apparent Hardness (HRC)	Micro Hardness (HRC)	T/R Strength (MPa)
FLC-4608 Modified	1120° C	Sinter Hardened and Tempered	7.2	35 40	60	1482
737 SFH	1120° C	Sinter Hardened and Tempered	7.15	39 41	60	2034
Ancorloy 2 (FD-0208)	1120° C	None	7.25	96 (HRB) 24	47	1834
FL-4405 HT	1120° C	Neutral Hardened - Quench and Tempered	7.3	43 44	59	1930
Wrought AISI 8620	N/A	Carburized – Quench and Temper	7.84	60	60	N/A

RESULTS

After testing, the cycle count was recorded and each gear was examined to determine the failure mode. This is a visual evaluation of the tooth surface for pitting, scuffing wear, or tooth breakage. The tested gears were also measured to assess changes in the tooth profile, and tooth lead geometry. Microstructures of the failures were also examined. Results as presented below.

FZG test results

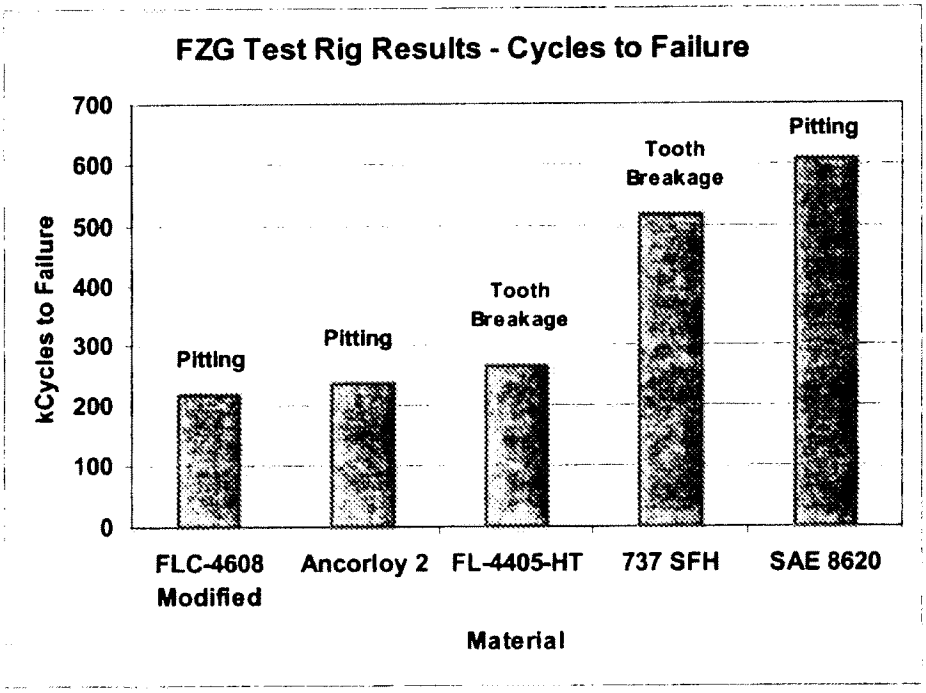


Figure 11: FZG Test results for each material as a function of cycles to failure

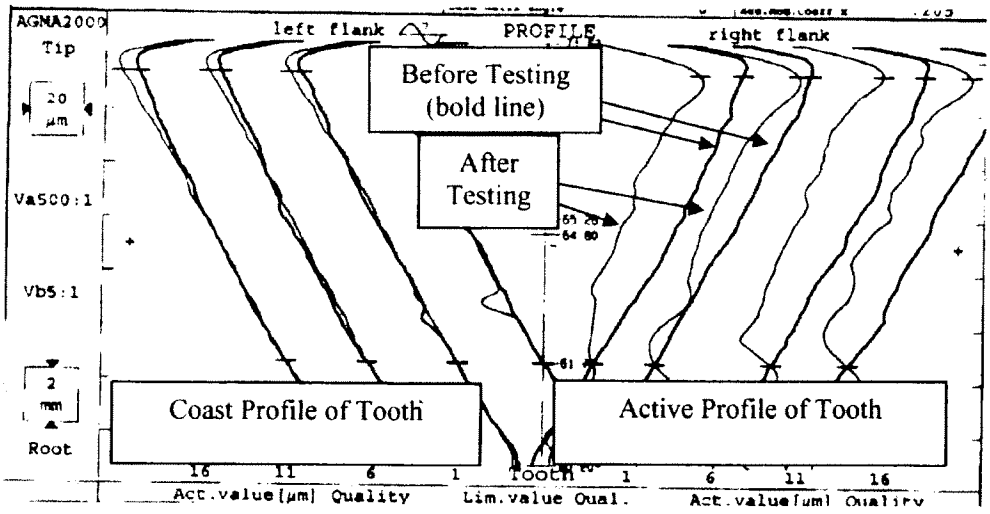


Figure 12: Tooth profile plot showing gear measurements before and after testing

The deformation of tooth flank in the profile direction is illustrated in Figure 12. This is indicative of plastic flow of material toward the tip of the gear. Similar changes in the gear profile after testing occur with gears that exhibit severe pitting. Notice the coast profile (non contact flank) shows little difference in profile measurement from before and after testing.

Microstructure evaluation

Figure 13 illustrates where the gears were sectioned for microstructural evaluation. The focus was the area adjacent to the pitch diameter where contact stresses were the highest.

Microstructure evaluations of the pitted P/M gears also exhibited plastic flow within the active profile. Interesting to note is that the addendum (tooth flank outside the pitch diameter) has opposite flow direction than the dedendum (tooth flank inside the pitch diameter). Because the tooth profile is positive i.e. there is no relief towards the tip, this area contacts furthest away from the pitch diameter and has the most sliding contact between the two gears. At the pitch diameter, there is nearly pure rolling contact that, in the microstructure, can be seen as an area with no flow on the tooth flank.

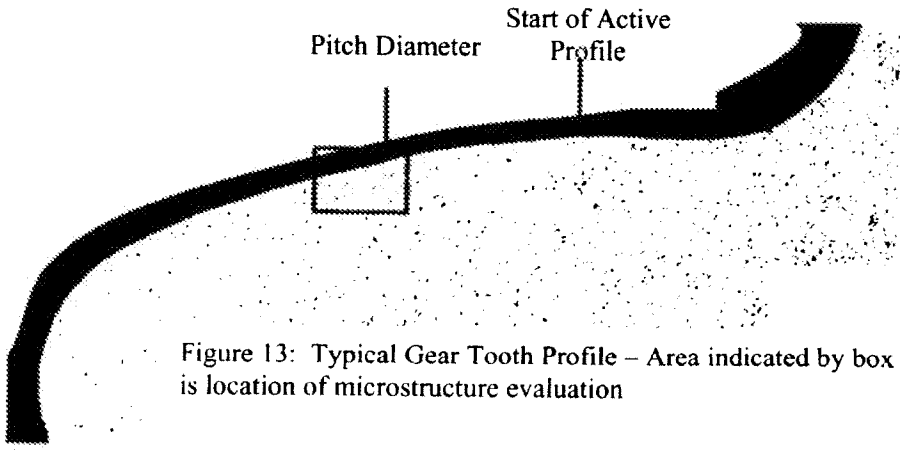


Figure 13: Typical Gear Tooth Profile – Area indicated by box is location of microstructure evaluation

Photos below show typical failed gear tooth microstructures (Figures 14-23).

FLC-4608 Modified

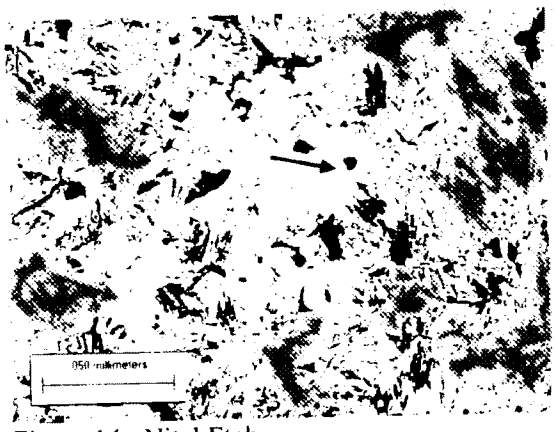


Figure 14: Nital Etch

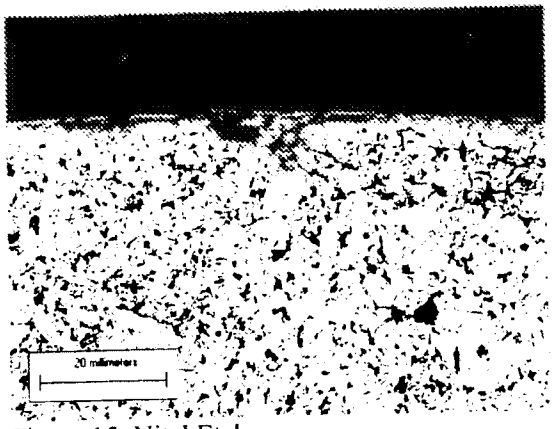


Figure 15: Nital Etch

The microstructure consists primarily of martensite, with areas of nickel rich regions indicated by arrows in Figure 14. Pores are normally distributed throughout the matrix. After 220 kCycles of testing the tooth surface exhibits plastic flow. Subsurface cracking is also common in the working area of the tooth flank. This is an indication of contact fatigue during the operation of the gear. The subsurface cracking observed is similar to previous publications which determined that nickel rich areas are prone to cracking from rolling contact fatigue[5,12].

Ancorloy 2

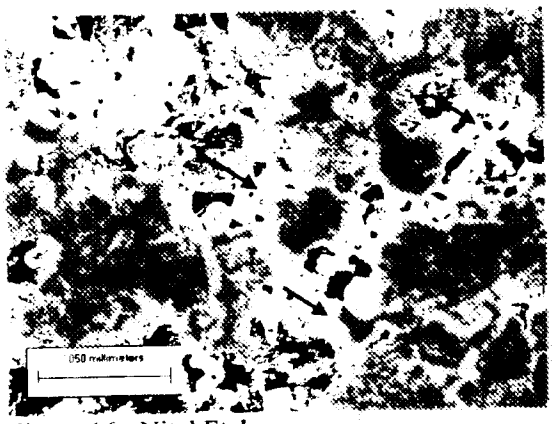


Figure 16: Nital Etch



Figure 17: Nital Etch – Arrows indicate flow direction.

The microstructure consists of a mixture of pearlite, martensite, and nickel rich regions. In Figure 16 the nickel rich areas are indicated by arrows. After 230 kCycles of testing, the samples show considerable surface densification, cracking of the surface, and spalling in the pitch line area. Evidence of plastic flow is observed on the surface. Arrows in Figure 17 indicate the direction of plastic flow. Once again, the subsurface cracking corresponds to previous information showing that nickel rich areas are prone to crack initiation during rolling contact fatigue. Another observation is the surface densification that was more evident in this material. This is considered plastic flow, which as discussed earlier, is a failure mode for gears.

FL-4405-HT

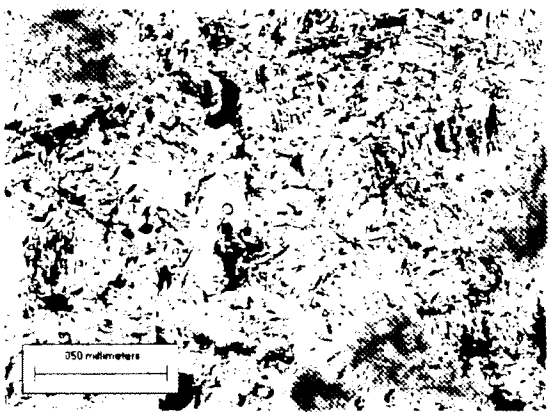


Figure 18: Nital Etch

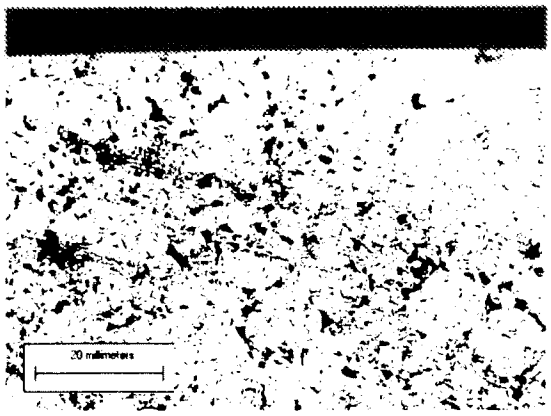


Figure 19: Nital Etch

Microstructure consists primarily of lath martensite with porosity normally distributed throughout the matrix. After 270 kCycles of testing, there was no evidence of surface or subsurface cracking. Pitting and plastic flow was not evident with this material, and the failure mode was tooth breakage.

737 SFH

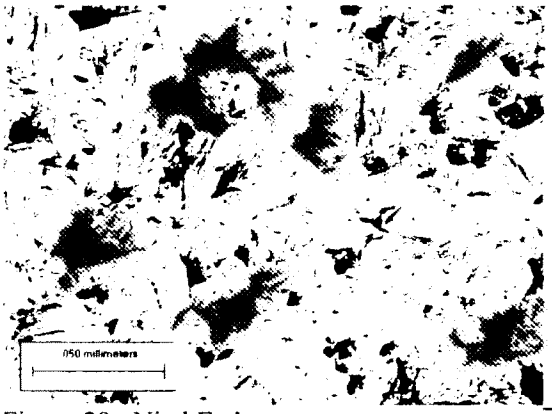


Figure 20: Nital Etch

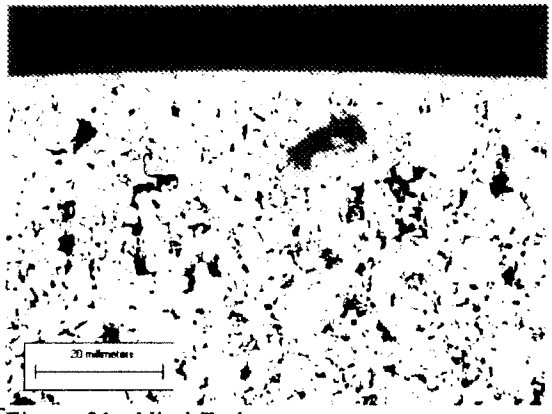


Figure 21: Nital Etch

Microstructure consists primarily of plate martensite with porosity normally distributed throughout the matrix. After 520 kCycles of testing, there was no evidence of surface or subsurface cracking. Of note is that no subsurface cracking was observed adjacent to the large pore in Figure 21. Pitting and plastic flow was also not evident with this material, and failure mode was tooth breakage.

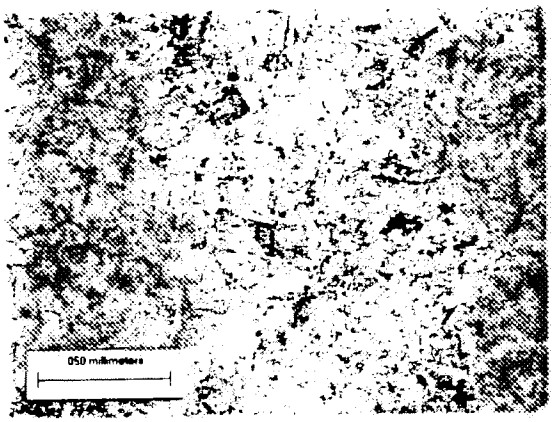


Figure 22: Nital Etch

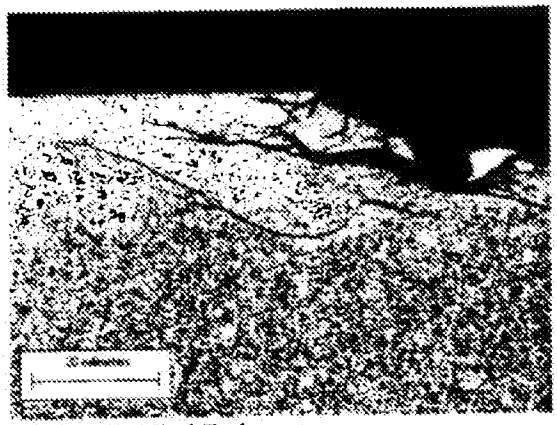


Figure 23: Nital Etch

Microstructure consists of fine martensite in the area of the carburized case as shown in Figure 22 above. The effective case depth is 700 μm to a hardness of 50 HRC. Figure 23 shows the surface of the tooth after 600 kCycles. The area shown is near the pitch diameter. This is a typical pitting failure of the test gears.

Conclusions

Based on the initial results, nickel rich areas in the microstructure are detrimental to pitting resistance. This is seen in the FLC-4608 Modified and Ancorloy 2 materials. Both of these samples have admixed nickel which during common sintering practices will not fully alloy in the matrix. Subsequently after sintering, these remaining areas are soft and much weaker than the martensitic matrix. Cracks most likely form in these weak areas and propagate to the surface causing the pitting failures seen on these samples. This is analogous to the results of previous papers[9,12] where nickel rich areas were prone to cracking when exposed to fatigue conditions.

Additionally, materials that contained admixed nickel exhibited extensive plastic flow in the active profile. Sintered hardened Ancorloy 2 exhibited more extensive plastic flow as well as distinctive surface densification likely due to its lower matrix hardness.

Another observation is that when admixed nickel was not present, the P/M gears did not exhibit pitting failures. This is seen in the results of the 737 SH and FL-4405-HT material tests. For these materials, the failures were due to tooth breakage, likely a result of tooth root fatigue. Microstructural evaluation did not discover either surface or subsurface cracks for either of these materials.

The notable difference in performance between FL-4405 HT and 737SH is not yet fully understood. 737 SFH has somewhat higher matrix strength, but was processed at a lower density. The higher carbon content of 737SH resulted in primarily a plate martensite structure with higher (estimated) amounts of retained austenite than FL-4405 HT. Finer lath martensite was observed in the FL-4405 HT. More investigation in needed into the performance of these two alloys.

Future Work

- FZG testing of gears made by other PM processes:
 - Surface densification
 - Powder forging
- Optimization of gear microstructures:
 - P/M compositions and alloying methods
 - Heat treatment processes
- Complete additional types of testing on the standard gear:
 - Single tooth bending fatigue
 - Impact
- Generate S-N curves for the most promising materials from each P/M gear manufacturing process
- Optimize root geometry to reduce stresses and thus increase the overall strength of the gears. This approach may lead to a root design that cannot be hobbed, but will outperform hobbed gears. With PM, there are many opportunities to improve in this area, at no cost to the customer.

REFERENCES

1. Townsend, D., *Dudley's Gear Handbook*, Second Edition. McGraw-Hill, Inc. 1992.
2. Morimoto, K. et al., *"Transmission spur gear powder forging"*, Proceedings of the 1973 International P/M Conference, MPIF/APMI, Princeton, NJ, 1973, Vol. 7, pp. 323-339.
3. Heuler, P., James, B., Lawcock, R., Schulz, H., Strömgren, M., and Wonneberger, R., *"The use of powder metallurgy for load bearing applications such as gears"*, R&D Report, German Federal Ministry of Education and Research (BMFT), 1988, December, Report-No. TF-2608 (COST 503)
4. Sanderow, H., "The Single Point Bending Fatigue Properties of P/M Steel Alloys", CPMT Project, Publication pending.
5. Dautzenberg, N., Lindner, K. H., and Strehl, R., *"Comparison of conventionally manufactured gears in single or double sinter process - technical and economical aspects"*, Proceedings of the PM World Congress, 1994, Vol. 1 , pp. 43-46
6. Rutz, H. G., and Hanejko, F. G., *"High density processing of high performance ferrous materials"*, International Journal of Powder Metallurgy, Vol. 31, No. 1, 1995, pp. 10-17

7. Donaldson, I., *"An Evaluation of High Performance Materials Processed by Warm Compaction"*, Advances in Powder Metallurgy & Particulate Materials, vol. 2, compiled by T.M. Cadle and K.S. Narasimhan, Metal Powder Industries Federation, Princeton, NJ, 1996, part 5, pp. 235-246.

8. Sandner, C.; Ratzi, R.; Lorenz, B., and Tobie, T., *"Sintered gears - achievable load-carrying capacities by conventional and new production methods"*, VDI-report no. 1665, VDI-Verlag, Düsseldorf, 2002, Vol. 1, pp. 295-310

9. Kotthoff, G., *"Neue Verfahren zur Tragfähigkeitssteigerung von gesinterten Zahnrädern"*, 2003, Ph. D. Thesis, Technical University Aachen, Germany, Shaker Verlag, Aachen, Bd.23/2003

10. Lipp, K., Sonsino, C.M., Pohl, D., and Hock, S., "Rolling Contact Fatigue Behavior if Sintered Steels- Endurable Hertzian Pressure and Damage Mechanisms", European Powder Metallurgy Conference, Granada, Spain, EPMA, Shrewsbury, UK, 1998, vol.3, p.143

11. Hoffman, G., Sonsino, C.M., and Michaelis, K., "Rolling Contact Fatigue – Component Design and Testing for P/M Applications", SAE Technical Papers Series, SAE 1999-01-0332, 1999

12. Sanderow, H. and McPherson, D., "The Rolling Contact Fatigue Properties of P/M Steel Alloys", Advances in Powder Metallurgy & Particulate Materials, Compiled by Volker Arnhold, Chiu-Lung Chu, William Jandeska, and Howard Sanderow, Metal Powder Industries Federation, Princeton, NJ, 2002, part 5, pp. 53-74.

13. Hoffman, G., Mandel, J., and Landgraf, C., "Effect of Pores and Porosity on Rolling Contact Fatigue of Sinter Hardened P/M Steel", Advances in Powder Metallurgy & Particulate Materials, compiled by Roger Lawcock and Mary Ann Wright, Metal Powder Industries Federation, Princeton, NJ, 2003, part 7, pp.299-313.

14. Krzan, B., and Vizintin, J, "Vegetable-based Oil as a Gear Lubricant", Gear Technology, July August 2003 pp 28-33.

15. ASM Committee on Failures of Gears, "Failures of Gears" ASM Handbook 8th ed., v 10, pp 507-524.

Rolling Contact Fatigue Performance Contrasting Surface Densified, Powder Forged, and Wrought Materials

William Jandeska
GM Powertrain
Pontiac, MI 48340

Richard Slattery
Capstan Atlantic
Wrentham, MA 02093

Francis Hanejko, Arthur Rawlings, Patrick King
Hoeganaes Corporation
Cinnaminson, NJ 08077

Presented at PM²Tec 2005
Montreal, Canada June 19 - 23

Abstract:

Previous experimental work demonstrated that rolling contact fatigue durability of high-density powder metallurgy samples was influenced by depth of surface densification (achieved via roll densification), sintering temperature, and heat treat practice. One observation of the previous work was reduced rolling contact fatigue life at high Hertz stress levels relative to wrought machined steel samples. There were also some questions regards the influence of nickel rich regions and how they affected rolling contact fatigue performance. In an effort to understand the influence of elemental nickel additions, FLN2-4405 samples were sintered at 2050 °F (1120 °C) and 2300 °F (1260 °C) and subsequently powder forged to full density. This experimental work was designed to clarify the effects of elemental nickel additions on rolling contact fatigue durability. Additionally, wrought AISI 8620 carburizing steel was machined into rolling contact fatigue samples, carburized and tested. Additionally, the AISI 8620 was evaluated for tensile, impact and fatigue characteristics in the quench and tempered condition.

Introduction:

Automotive powertrain requirements necessitate that individual components have mechanical properties adequate to insure system reliability up to 250,000 kilometers. [1] Multiple requirements of high static strength, bending fatigue, and rolling contact fatigue durability led gear designers to utilize forged and machined wrought steels to ensure long-term vehicle reliability. Although P/M offers lower component cost, fatigue limitations of conventional press and sintered components precluded P/M utilization in these demanding applications. Considerable research work is underway to explore the possibility of using high density P/M in applications traditionally fulfilled by wrought steels. [2,3,4,5] Specifically, advanced processing utilizing high core densities combined with selective surface densification may produce

components with nearly equivalent surface fatigue durability and core strengths suitable for these high strength applications.

Prior experimental work demonstrated rolling contact fatigue life of P/M is dependent upon amount of surface porosity, depth of densification, and microstructural features such as type of martensite formed and secondary phases such as nickel rich areas. [2] Selectively densified P/M materials are strongly affected by the rolling contact fatigue stress level. Specifically, at Hertzian stresses at and below 1900 MPa, selectively densified P/M material exhibit rolling contact fatigue life equivalent to wrought steels. However, at Hertzian stresses approaching 2500 MPa, surface densified P/M materials had lower rolling contact fatigue life compared to wrought steels. In an effort to answer questions concerning influence of surface porosity, depth of carburized layer and effects of nickel rich regions prompted this investigation of full density P/M materials to potentially clarify these issues.

As noted earlier, surface densified P/M materials showed equivalent rolling contact fatigue life to wrought steels at contact stresses of 1900 MPa and below. However, increasing demand for higher engine performance and smaller gears sizes place even greater performance demands on gear materials. To understand Hertzian stresses within gears, it useful to go through a typical contact stress calculation of a gear. Assume a gear with a 20° pressure angle and a Modulus of Elasticity of 30 million psi (206,000 MPa); the maximum compressive stress can be calculated according the following equation:

$$s_c = 5715\sqrt{\frac{W_t}{Fd}\left(\frac{m_G + 1}{m_G}\right)} \qquad \{1\} \text{ [Reference 6]}$$

In which

- Sc = surface compressive stress in psi
- W_t = driving pressure in pounds = pinion torque/pitch radius
- F = face width in inches
- d = pitch diameter in inches
- m_G = ratio of gear teeth to pinion teeth
- Ss = Maximum subsurface shear stress in psi

In addition to surface compressive stresses, there exists a maximum shear stress, which is calculated to be

$$Ss = 0.295\ Sc \qquad \{2\} \text{ [reference 6].}$$

This maximum compressive shear stress occurs at a depth below the surface equal to approximately 0.40 times the bandwidth of contact. As an example, assume that an engine develops 250 ft-lbs of torque and this torque is transmitted through the pinions (load sharing between two pinions) with a pitch diameter of 1.500 inches, a face width of 1.000 inch and a final reduction ratio of 3.3 to 1, then the calculated stresses from equation {1} and equation {2} are as follows:

- Maximum Hertzian stress, Sc ~180,000 psi (1240 MPa)
- Maximum Sub surface shear stress, Ss ~55,000 psi (380 MPa)
- Depth of maximum shear ~0.009 inches (0.23 mm)

However, torque spikes because of adverse driving conditions or higher "m_G" values associated with lower gear ratios, these maximum Hertzian and shear stresses can increase to greater than 150% of the values listed. Along with greater surface contact stress, the depth of maximum shear would increase approximately 40%. Thus for P/M to successfully replace wrought steel in these high strength applications, P/M processing must meet or even exceed the performance of current gear materials.

Experimental Procedure:

Sample Preparation:

To understand the effects of nickel rich regions on rolling contact fatigue of P/M materials, an FLN2-4405 premix was prepared and samples were compacted to a nominal 6.8 g/cm³ density (preform dimensions 3.5 inch OD x 1.25 inch tall). Half of these samples were sintered at 2050 °F (1120 °C) and half were sintered at 2300 °F (1260 °C). After sintering, all samples were powder forged to ~100% pore free density (forged dimensions 4.0 inch OD x 1.0 inch tall) using a forging temperature of 1800 °F (980 °C). After forging, rolling contact fatigue samples were machined avoiding any powder-forged surface. Once machined, samples were vacuum carburized at 1700 °F (925 °C) for 3 hours, utilizing a 90 minutes boost cycle and a 90-minute diffuse cycle. Quenching was done with high-pressure nitrogen gas. All samples were then tempered at 400 °F (205°) for 1 hour. Carburizing was targeted to produce a 0.9 to 1.0% surface carbon after the boost phase. After carburizing, grinding of the ID was done to achieve the desired outer diameter to inner diameter concentricity.

In order to understand the effects of carburizing practice on rolling contact fatigue life, forging quality AISI 8620 wrought steel was machined into rolling contact fatigue samples. These wrought samples were carburized at the same time as the FLN2-4405 samples. Additionally, the AISI 8620 material was machined into tensile, impact and rotating bending fatigue samples. These test specimens were tested according to MPIF standards.

Rolling Contact Fatigue Testing

As described in previous reports, rolling contact fatigue testing was performed using a ZF-RCF test bench. [2,7] Benefits of this screening method are as follows:

- Ability to test heat treated surface of component
- Line contact for applied Hertz stresses
- Full elasto-hydrodynamic lubrication thus focusing on material properties without interference from surface pitting phenomena.
- Ability to incorporate sliding into test regime
- Relatively short test times to accelerate evaluation.

Test conditions for the ZF rolling contact fatigue test bench were as follows:

- Test speed of 3000 RPM, 9000 load cycles per minute
- Two load levels: 1900 / 2000 MPa and 2500 MPa, assuming a Young's Modulus of 30 million psi (206,000 MPa), loading constant.
- Sliding of -24% between the test sample and load wheels.
- Lubricant: Dextron III, automatic gear box oil provided by General Motors Corporation, the oil was held at 80 °C ± 2 °C.

- Failure during the rolling contact fatigue test was detected using an accelerometer, which detected excessive vibration from the surface spalling of the sample
- Five samples were evaluated at each Hertzian stress level. The probability of survival was calculated according to the following
 - $Ps = ((3m-1)/(3n+1)) * 100\%$ {3}

Results:

Rolling Contact Fatigue Testing

Rolling contact fatigue test results of powder forged FLN2-4405 and AISI 8620 are presented in Table 1. Test results are shown for Hertzian stress level, B50 life to failure, a ratio of B10 to B90 lives, plus the slope of the S-N curve. These properties are defined as follows:

- B50 — 50% statistical survival life, based on equation 3
- B10 — 10% statistical survival life, based on equation 3
- B90 — 90% statistical survival life, based on equation 3
- Slope of S-N Curve — Calculated slope of low cycle fatigue portion of S-N curve

Table 1
Rolling Contact Fatigue Live of Samples Evaluated

Material / Sinter Condition	Hertz Stress Level, MPa	B50 life, x 10^6 cycles	Ratio of B10 / B90 lives	Slope of S-N Curve
FLN2-4405 / 1120 °C	1900	13.0	1 : 1.9	6.5
	2500	2.1	1 : 1.9	
FLN2-4405 / 1260 °C	2000	13.0	1 : 2.6	8.0
	2500	2.1	1 : 1.9	
AISI 8620	2000	20.0	1 : 1.8	7.0
	2500	4.2	1 : 2.7	
AISI 5120*	1900	16.0	1 : 1.8	3.5
	2500	6.1	1 : 1.7	

* AISI 5120 was tested in previous study.

A note about the data presented in Table 1. Both AISI 8620 and FLN2-4405 (sintered at 2300 °F [1260 °C]) were evaluated at a lower stress level of 2000 MPa. This deviation in test procedure was done because initial sample testing exceeded 50 million cycles prior to failure (considered a run out). In order to develop meaningful B10, B50 and B90 lives, the contact stress level was increased to 2000 MPa. Data documenting rolling contact fatigue life of AISI 5120 was developed in a separate program.

Mechanical Property Data

Mechanical property data for AISI 8620 was determined in both the principal working direction (longitudinal) and perpendicular to the principal working direction (transverse). Often data for

wrought steels is quoted for the longitudinal direction only. However, depending on the type of gearing, applied gear loading could be completely in the transverse direction (spur gears) or some vector function of both longitudinal and transverse properties (helical gears). All samples were machined from hot rolled round bar stock, austenitized at 1700 °F (925 °C), oil quenched and tempered at 400 °F (205 °C). Table 2 presents the data developed for the AISI 8620 material.

Table 2
Mechanical Properties of Q&T AISI 8620 and FLN2-4405 at 7.40 g/cm³ Core Density

Property	AISI 8620		P/M at 7.40 @ g/cm³ *
	Longitudinal	Transverse	
Yield Strength Q&T, 10^3 psi (MPa)	156 (1075)	154 (1070)	180 (1240)
Ultimate Tensile Strength Q&T, 10^3 psi (MPa)	197 (1355)	193 (1330)	210 (1445)
Tensile Elongation, %	8.0	6.1	1.0
Q&T Hardness, HRa	70.6	69.3	81
Impact Notched, ft.lbf (Joule)	27 (37)	10 (14)	N/A
Impact Unnotched, ft.lbf (Joule)	230 (312)	227 (227)	13 (18)
50% Fatigue Endurance Limit Carburized, 10^3 psi (MPa)	71 (490)	54 (370)	59 (405)

* Data from MPIF Standard 35 [8]

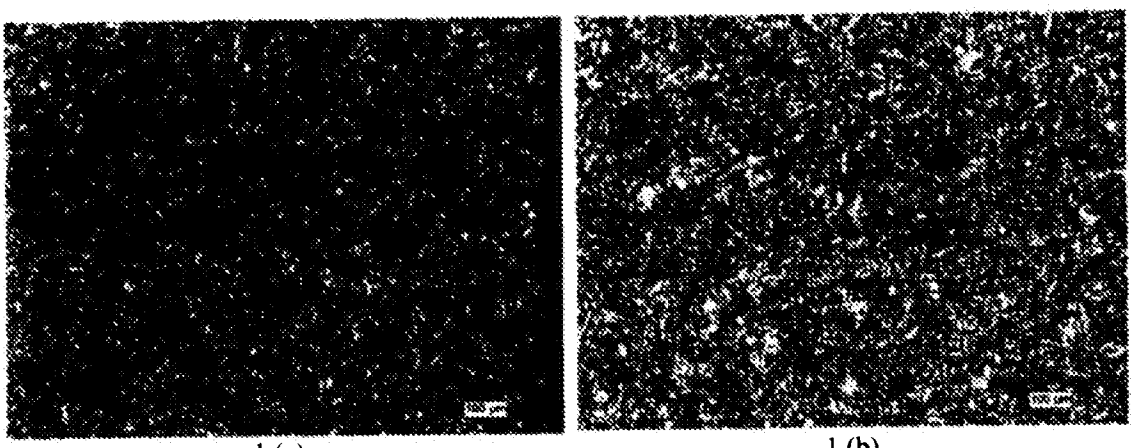
Discussion:

Rolling Contact Fatigue

Rolling contact fatigue results presented in Table 1 indicate that carburized AISI 8620 evaluated in this summary showed superior rolling contact fatigue performance relative to AISI 5120 at 2000 MPa contact stress. Similarly, powder forged FLN2-4405 sintered at 2300 °F (1260 °C) also showed superior life to the base line AISI 5120 material at 2000 MPa. However, FLN2-4405 sintered at 2050 °F (1120 °C) and subsequently powder forged had rolling contact fatigue life ~20% lower than the base line AISI 5120 material. Rolling contact fatigue performance at 2500 MPa was significantly different; all materials evaluated in this study showed rolling contact fatigue life lower compared to AISI 5120. This result was unexpected because previous testing by Chen etal. showed that AISI 8620 material had rolling contact fatigue life equal to or superior to the AISI 5120 steel. [9]

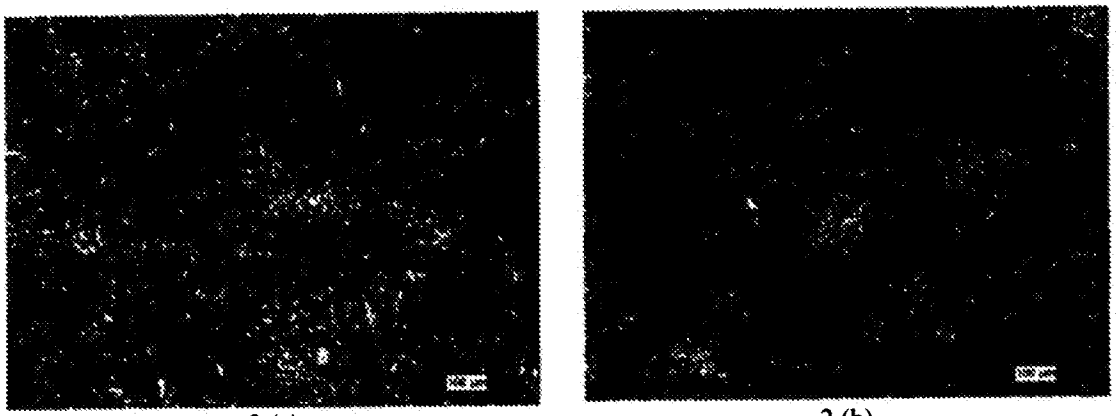
To investigate potential reasons for the difference in rolling contact fatigue behavior at 2500 MPa, all samples were examined metallographically. Case and core microstructures of the three materials are presented as Figure 1 through Figure 3. Total case depth for each material is approximately 800 microns. AISI 8620 has a low carbon martensitic core with a well-defined boundary between case and core microstructure. The carburized case microstructure shows an acicular type martensitic structure with evidence of retained austenite. The core is essentially a low carbon martensitic microstructure. Both powder-forged samples show a case microstructure containing acicular martensitic with evidence of retained austenite. Core microstructures of the powder-forged samples are predominantly lath type martensite. As expect, powder forged

samples sintered at 2050 °F (1120 °C) show relatively large islands of nickel rich regions. High temperature sintering completely diffused the elemental nickel addition thus providing a homogeneous microstructure.



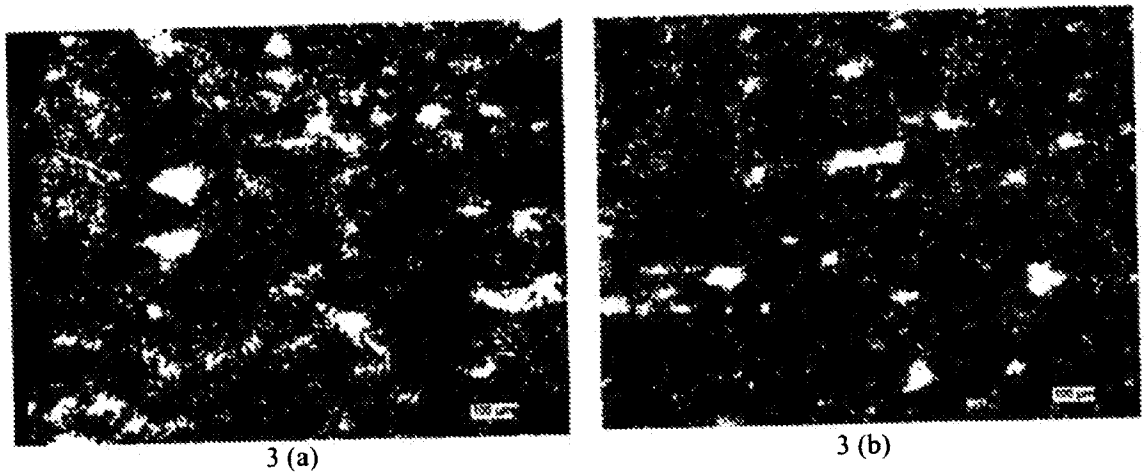
1 (a) 1 (b)

Figure 1: Case and Core Microstructure of AISI 8620 Rolling Contact Fatigue Samples in Carburized Condition



2 (a) 2 (b)

Figure 2: Case and Core Microstructure of FLN2-4405 Rolling Contact Fatigue Samples sintered at 2300 °F (1260 °C) in Carburized Condition

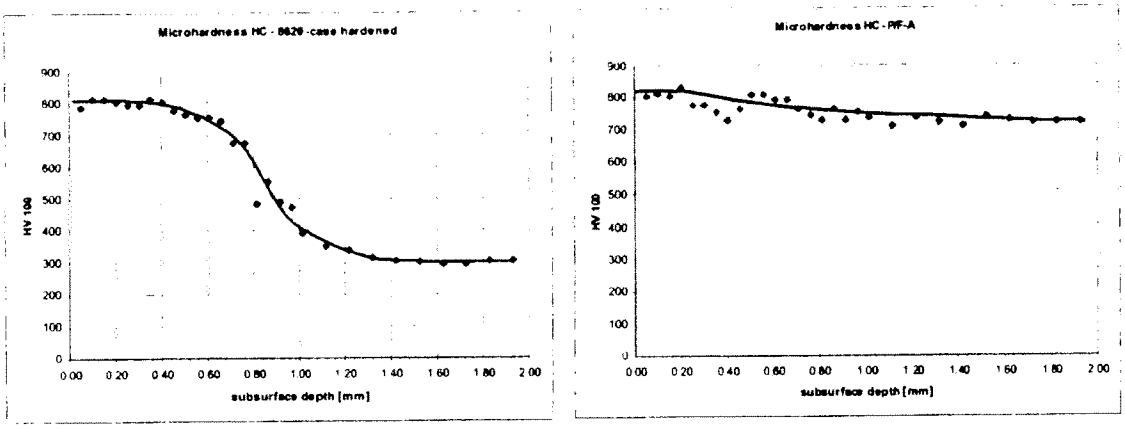


3 (a) 3 (b)

Figure 3: Case and Core Microstructure of FLN2-4405 Rolling Contact Fatigue Samples sintered at 2050 °F (1120 °C) in Carburized Condition

Reviewing the metallographic analysis, all microstructures are typical of carburized steel with a ~1.0% surface carbon. There was no decarburization or grain boundary carbides at the surface. What was troublesome about these results was the difference is rolling contact fatigue of AISI 8620 at 2500 MPa compared to previously tested AISI 5120 wrought steel. Differences in rolling contact fatigue performance may relate to the carburizing cycle. All samples in this study were carburized were done via a single boost / diffuse cycle; that is, test samples were held at 1700 °F (925 °C) for 90 minutes in a carburizing gas. Following this carbon boost stage, all samples were then held at 1700 °F (925 °C) for 90 minutes to diffuse the high surface carbon. Recent conversations with gear designers indicated that vacuum carburizing techniques for gearing utilize multiple boost / diffuse cycles. [10] This multiple boost / diffuse processing produces a more uniform carbon distribution through out the carburized case. Having a more uniform carbon distribution in the carburized layer would yield higher strength through out the case and potentially give greater surface compressive stresses deeper in the carburized layer. Testing at high Hertz stresses will produce higher subsurface shear stresses, thus a more uniform carburized layer would produce better performance.

Figure 4 shows the micro-hardness traverse of these samples. AISI 8620 shows a defined case / core hardness. Because of the high core carbon of the powder forged FLN2-4405, it behaves more like a through hardening material. These hardness traverses indicate that the AISI 8620 material may possess greater surface compressive stresses relative to the FLN2-4405 materials. This could be a partial explanation for the difference in rolling contact fatigue performance.



4 a 4 b

Figure 4: Microhardness Traverses of Samples Evaluated
4 a Carburized AISI 8620
4 b Carburized FLN2-4405

Analysis of the pitting showed differences between the AISI 8620 and the powder forged samples. Generally, pitting of AISI 8620 samples was mostly subsurface originating at the depth of maximum subsurface shear stress (see Figure 5). Both powder forged samples seemed to have a greater tendency for crack initiation at the surface which then proceeded into the core material (Figure 6). There was also evidence of deep subsurface cracking at depths below the depth of maximum shear stress (Figure 7). Differences in microhardness profiles suggest that the powder-forged samples more closely resemble a through-hardened material and therefore should possess lower rolling contact fatigue life. [11]

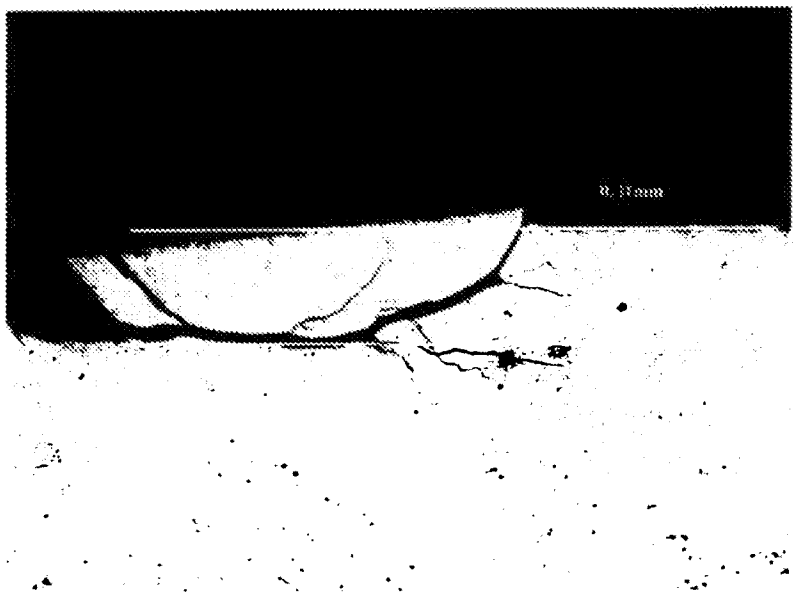


Figure 5: Subsurface cracking observed in carburized AISI 8620, sample evaluated at 2500 MPa.

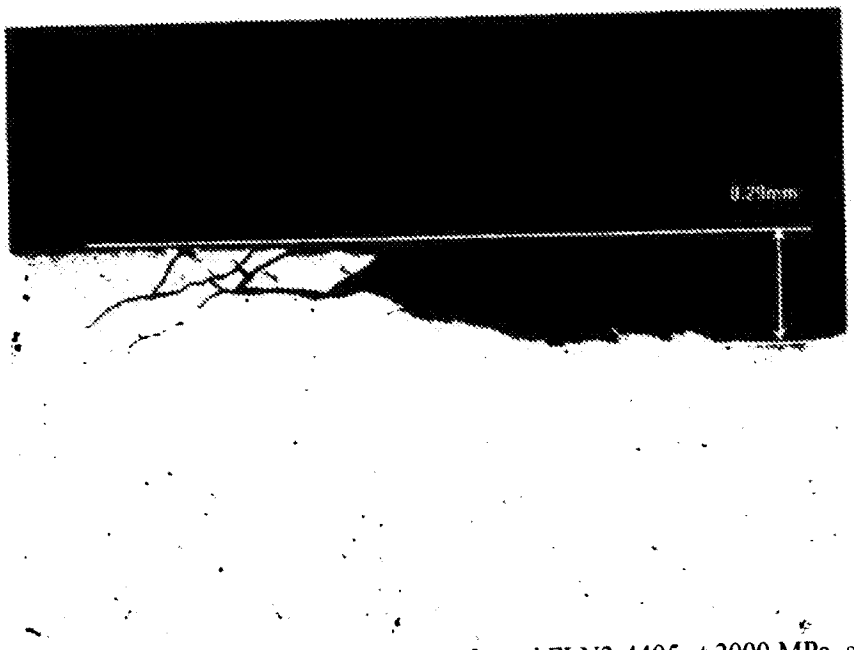


Figure 6: Surface cracking observed in powder forged FLN2-4405 at 2000 MPa, sintered at 2300 °F (1260 °C)

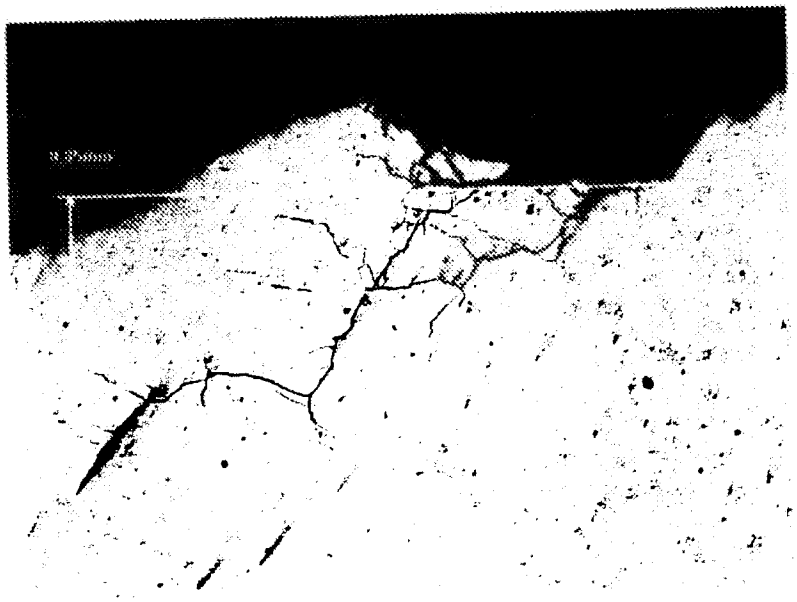


Figure 7: Deep subsurface cracking associated with powder forged FLN2-4405 material, 2500 MPa material sintered at 2300 °F (1260 °C)

One objective of this experimental work was to compare the rolling contact fatigue performance of powder forged FLN2-4405 to surface densified FLN2-4405. Data for both processing

conditions is shown in Table 3. B50 rolling contact fatigue life for surface densified FLN2-4405 for both sintering conditions are equivalent to powder forged FLN2-4405 at the 1900 / 2000 MPa Hertz contact stress. Surface densified FLN2-4405 sintered at 2050 °F (1120 °C) has greater scatter in test data as noted by the B10/B90 ratio. However, high temperature sintering of FLN-4405 coupled with surface densification reduces test scatter to nearly the same as the powder forged samples and approaching the scatter of the wrought steels. Again, it is that B50 life at 1900 / 2000 MPa of either surface densified or powder forged FLN2-4405 are equal to the AISI 5120 baseline material. Rolling contact fatigue at 2500 MPa is reduced relative to AISI 5120 bales. Reiterating, this reduction in rolling contact fatigue life at 2500 MPa was also noted for AISI 8620. This reduction may result from differences in carburizing practice and subsequent level and depth of residual surface compressive stresses.

Table 3
Results of earlier Rolling contact fatigue Testing of Surface densified FLN2-4405

Material / Sinter Condition	Hertz Stress Level, MPa	B50 life, x 10^6 cycles	Ratio of B10 / B90 lives	Slope of S-N Curve
2050 °F (1120 °C) SD	1900	17.0	1 : 10	6.5
	2500	2.6	1 : 4.8	
2300 °F (1260 °C) SD	1900	10.0	1 : 2.0	4.6
	2500	2.8	1 : 3.2	
2300 °F (1260 °C) SD and annealed	1900	19.0	1 : 3.0	9.0
	2500	1.7	1 : 2.5	
Powder forged / 1120 °C	1900	13.0	1 : 1.9	6.5
	2500	2.1	1 : 1.9	
Powder forged / 1260 °C	2000	13.0	1 : 2.6	8.0
	2500	2.1	1 : 1.9	
AISI 8620	2000	20.0	1 : 1.8	7.0
	2500	4.2	1 : 2.7	
AISI 5120	1900	16.0	1 : 1.8	3.5
	2500	6.1	1 : 1.7	

Relative to the effects of nickel rich regions resulting from elemental nickel additions, testing of powder forged FLN2-4405 verified the crack initiation and propagation nature of these microstructural phases. Figure 8 [2] showed cracking emanating from residual porosity within the locally densified surface region. In this earlier work, the effects of elemental nickel are quite dramatic from the failure analysis. In this SEM photomicrograph, the cracking follows areas of nickel rich microstructural features. Residual porosity in these areas occurs because of differences in strength of the various microstructural elements. In regard to the powder-forged samples of FLN2-4405, no evidence of residual porosity adjacent to nickel rich regions was found. Therefore, the assumption that the reduction in rolling contact fatigue life occurs because of these regions is determined empirically. However, nickel rich regions within the microstructure represent areas of areas of lower strength. Because of the subsurface stress characteristics of rolling contact fatigue, these low strength regions can result in potential sites for crack initiation and propagation.

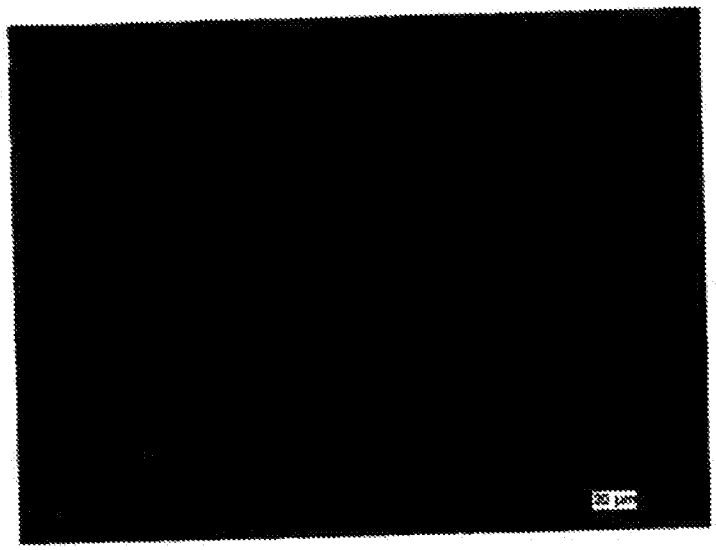


Figure 8: Crack propagation through nickel rich regions of surface densified material.

Mechanical Property Test Results

Mechanical property testing of AISI 8620 showed a marked directionally in both fatigue and impact properties. Tensile testing did not show the same degree of directionality except for the elongation value. All testing was done on machined round samples. The reduction in fatigue and impact from longitudinal to transverse varied from approximately 40% for the carburized fatigues to greater than 50% for the notched impact samples. Un-notched impact testing did not show the degree of reduction from longitudinal to transverse.

Directionality is important because many gears (spur gears) are actually loaded perpendicular to the principal working direction. Helical gears are loaded in both directions depending upon the helix angle of the gear (a 20% helical gear has the majority of its loading in the transverse direction). Often in literature databases, mechanical properties cited are longitudinal values with almost no mention of the transverse properties. Unlike wrought steels, P/M components are isotropic. There is some reduction in properties at the neutral axis of the part because of the reduction in density at this zone; however, with advanced part processing the reduction in density at the neutral zone is significantly reduced. Referring to Table 2, P/M offers nearly identical yield and tensile strengths but elongation and impact values are much reduced compared to wrought steels. Nearly equivalent rolling contact fatigue properties can be obtained through proper choice of alloy and processing condition.

Fatigue values shown in Table 2 were generated using rotating bending fatigue samples. Modified single gear tooth bending fatigue shown values nearly equivalent to the tensile strength of AISI 8620 material. [12] It is important to note that this disparity is a function of the test bar geometry and test conditions.

Conclusions:

1. Rolling contact fatigue testing of powder forged FLN2-4405 demonstrated that elemental nickel additions are detrimental predominantly in surface densified material. Although elemental nickel does not lower the B50 life, the amount of scattering in life is greater. This greater scattering results from the residual porosity inherent with these phases and subsequent crack initiation and propagation tendencies for these phases. High temperature sintering does homogenize the elemental nickel additions thus promoting superior rolling contact fatigue life at lower contact stresses.
2. Rolling contact fatigue testing of AISI 8620 produced superior life at 2000 MPa relative to the baseline AISI 5120 material. However, testing at 2500 MPa showed the baseline material to have superior rolling contact fatigue life. This difference is related to the carburizing cycle employed.
3. It is desirable to use a lower carbon P/M material for gearing applications. A lower core carbon promotes enhanced surface densification and better case / core properties resulting from carburizing.
4. Comparison of powder forged FLN2-4405 to surface densified FLN2-4405 showed nearly identical rolling contact fatigue life at both high and low stress conditions. This indicates that surface densification may be an acceptable method to achieve nearly wrought properties provided subsequent heat treatments are identical.
5. Mechanical property testing of AISI 8620 material showed marked directionality from the longitudinal to the transverse direction. This directionality is greatest in fatigue and impact performance. P/M offers less directionality in properties.

References:

1. M. LeGault and J. Collins, "P/M Components in Heavy Duty H2 Transfer Case", SAE Paper # 2004-01-0487.
2. William Jandeska, Richard Slattery, etal, "Rolling Contact Fatigue of Surface Densified FLN2-4405", International Journal of Powder Metallurgy, Volume 41, Issue 3, 2005, pp. 49 –61.
3. R. Shivanath, etal, Vacuum Carburizatin of High Performance Automotive PM Parts, Industrial Heating, August 2003.
4. L. Sigl, G. Rau, M. Krehl, "Properties of Surface Densified P/M Gears" SAE Paper # 2005-01-0711.
5. V. A. Denise, etal, "Surface Densification of PM Materials", Advances in Powder Metallurgy and Particulate Materials – 2000, Metal Powders Industry Federation, Princeton, NJ 08540 pp. 3-127 to 3-137.
6. Darle Dudley, "Handbook of Practical Gear Design", p 2-14, McGraw-Hill Book Company, 1984.
7. K. Lipp, G. Hoffmann, "Design for Rolling Contact Fatigue", Advances in Powder Metallurgy and Particulate Materials – 2002, Metal Powder Industries Federation, Princeton, NJ, 08540 pp.5-28 to 5-51.
8. MPIF Standard 35, 2003 Edition, Metal Powders Industry Federation, Princeton NJ.
9. Joe Chen, John Flynn, Geoff Semrau, "Gear Surface Durability Development to Enhance Transmission Power Density", Gear Technology, July / August 2002, pp. 20-25.
10. R. Leachman, Private Communication
11. H. Sanderow, "Final Report, Rolling Contact Fatigue (RCF) Test Program", Prepared by the Center for Powder Metal Technology (CPMT), September 2001.
12. www.Mat web.com.